Investigation of CW and LFM waveforms for Bi- and Multistatic Radar Synchronisation

Lucas L. Lamberti^{#1}, Stefan V. Baumgartner^{#2}, Gerhard Krieger^{#3},

*Microwaves and Radar Institute, DLR, Germany

{¹lucas.lamberti, ²stefan.baumgartner, ³gerhard.krieger}@dlr.de

Abstract — Multistatic radar systems have long been of great interest to a wide range of applications. Due to the uncoupled local oscillators in each radar, synchronisation of the radars is necessary to perform coherent processing of the data. Considering the use of synchronisation signals independent from the signals used for the radar operation, this paper analyses the estimation performance of Continuous Wave (CW) and Linear Frequency Modulated (LFM) waveforms when their parameters such as bandwidth, frequency, and duration are varied. Effects of synchronisation errors are shown for Synthetic Aperture Radar (SAR) imaging, however the synchronisation concepts are not exclusive to SAR.

Keywords - synchronisation, fmcw, synthetic aperture radar, multistatic.

I. Introduction

Synchronisation of distributed radar systems plays a key role in coherent data processing, especially for multistatic SAR imaging, interferometry, and tomography [1]. For an Unmanned Aerial Vehicle (UAV) based multistatic radar system, each radar is carried on a different UAV platform and they are each driven by their own Local Oscillator (LO) frequency reference. Figure 1 shows a bistatic example constellation. Due to hardware tolerances in the oscillators on each radar unit, relative offsets such as frequency and timing offsets, as well as incoherent phase noise lead to deteriorations in the imaging as shown in [2]. These offsets do not cancel out like in monostatic systems and have to be compensated either during operation or afterward.

This problem has been widely studied in literature as it plays an important role in distributed radar networks and communication systems. To this end, different methods have been presented. In [3], timestamps are transmitted between the radars to synchronise the timing via the principle of a Two Way Time Transfer (TWTT). Similar time transfer methods have been used for radar networks in [4, 5]. A different approach is the transmission of the radar waveform itself as a reference in the bistatic receiver, e.g., via the sidelobes or a dedicated channel [6-13]. While most of them rely on a bidirectional synchronisation exchange, the method in [9] synchronises only the receiver to a master via a one-way signal. Another approach is to use the multistatic receivers merely as repeaters to the transmitter, where the processing will be done. This has been proposed as MirrorSAR in [14]. A similar approach was demonstrated in [15]. Lastly, synchronisation purely via Global Positioning System (GPS) is proposed in [16].

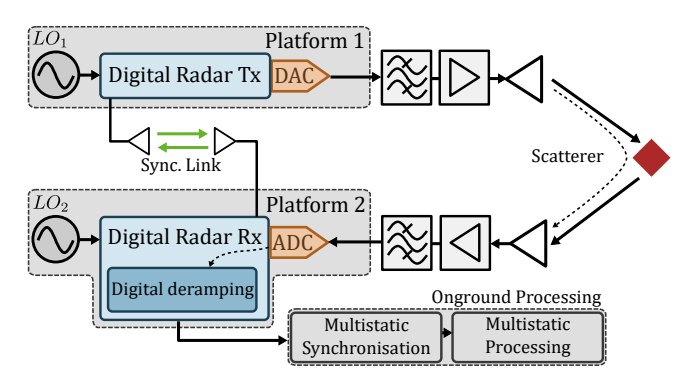


Fig. 1. Bistatic concept of two digital radar units with radar- and synchronisation subsystem on the same chip. In this example, radar platform 1 acts as the transmitter and radar 2 as the bistatic receiver.

Advances in semiconductor manufacturing have brought the emergence of direct Radio Frequency (RF) transceiver systems to the market [17], offering a higher degree of flexibility regarding the waveforms used for radar and synchronisation. Radar and synchronisation links may operate simultaneously with different waveform parameters or entirely different waveforms. Viewing the synchronisation waveform independently, this paper analyses the impacts on synchronisation performance, i.e., the estimation of relative offsets between stations, when waveform parameters such as frequency, bandwidth (in the LFM case) or duration are changed. Moreover, contrary to most literature in the field the time-bandwidth products considered here are quite large, with chirp durations and bandwidths of up to 1 ms and 2 GHz, respectively, leading to effects that are often neglected for small bandwidth signals.

Section II outlines the modulation and simulation approach, as well as the method used to estimate the synchronisation errors from the exchanged waveforms. In Section III the simulation results are shown and discussed. The paper is concluded in Section IV.

II. SYNCHRONISATION ERRORS AND SIMULATION

To simulate the radar echos and synchronisation waveform exchange, a bistatic Frequency Modulated Continuous Wave (FMCW) radar is assumed as shown in Figure 1. Both stations are simulated to be carried by a UAV with a linear flight trajectory. To focus on the LO induced errors, both stations are simulated to be in the same location with no relative velocity between each other. The LO offsets between both stations are modeled assuming a constant frequency offset over the data

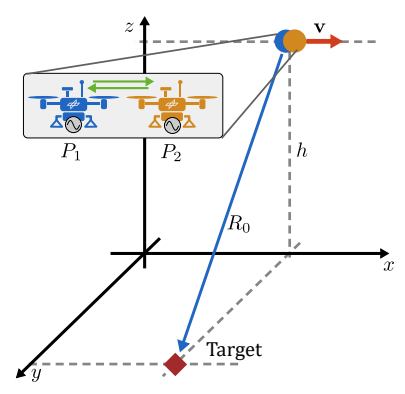


Fig. 2. Geometric simulation setup of two colocated, UAV-carried FMCW radar units P_1 and P_2 moving with velocity vector \mathbf{v} . The green arrows symbolize the bidirectional synchronisation signal exchange.

take duration. This offset results in carrier frequency errors, a timing drift of the Pulse Repetition Interval (PRF), and differences in the sweep rate of the LFM [10, 11]. Additionally, incoherent phase noise is modeled that varies from chirp to chirp [2, 6].

To estimate the LO offsets, synchronisation waveforms are periodically exchanged between both stations, recorded and processed afterward. The sampling frequency of the signals stored to memory is assumed sufficiently high, such that no range folding occurs due to the erroneous time drift. This will in praxis be assured by periodical resetting of the local time counters with a GPS 1-Pulse Per Second (PPS) signal. A visualisation of the simulation scene is shown in Figure 2.

The radar and synchronisation signal models follow the common derivation for LFM and CW waveforms, similar to [10] and [6]. The incoherent LOs will cause a carrier frequency offset, a slow-time varying timing offset of the PRF, since local time counters are diverging over time, and incoherent phase noise. As a result, the focused radar signal will experience an erroneous range shift and a smearing of the main lobe in both range and azimuth direction. All those errors are related to the LO frequency offset, which in turn drives the clocking of the radar. The relative deviations between both stations are summarised as:

- Carrier frequency offset, causing a range error
- Ramp rate offset, causing a range error and a range-peak smearing due to a quadratic phase error.
- Timing offset, which includes an initial start time offset and a time drift increasing from chirp to chirp, leading to a shift in range
- Phasenoise difference, leading to a shift and defocusing
 of the peak in azimuth direction, as well as residual
 phase noise in the peak that negatively impacts
 applications like interferometric imaging.

By tracking the range peak of multiple FMCW synchronisation signals and evaluating the signals received in both stations, the time drift can be estimated, from which correction parameters can be obtained similar to [10, 11].

It is important to briefly outline this estimation process. First, the range compression is performed for all received synchronisation up- and down LFM beatsignals via a

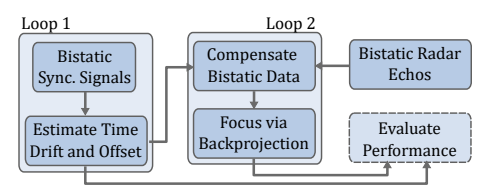


Fig. 3. Simplified simulation processing block diagram.

zero-padded Fast Fourier Transform (FFT). After locating the peak, a fine peak frequency estimate is obtained via a Quadratic Least Squares (QLS) parabolic fit [4], yielding a linear function for both stations. By computing the difference, the relative time drift can be obtained, which concludes the estimation process. This is done for up- and down chirps separately and the average of both is considered for the analysis in Section III.

The compensation of the radar receive echoes is then done based on those estimations, and the quality in turn depends on the estimation of these parameters. This paper investigates this parameter estimation quality when the waveform parameters are varied, and how they translate to quality degradations in the SAR focused image. SAR processing involves the compression of the radar echoes not only in range but also in azimuth direction, i.e., along the flight track of the simulated UAVs. While the range compression is done via the FFT as typical for FMCW radar [18], the azimuth compression is achieved via the backprojection algorithm [19]. For the performance analysis, range and azimuth cuts are extracted from the final bistatic image Impulse Response Function (IRF) and the quality is analyzed by means of the 3dB mainlobe width as well as range and azimuth peak to sidelobe ratio. The full simulation and evaluation pipeline is shown in Figure 3 and follows these steps:

- 1) Simulate the synchronisation waveform exchange for the whole operation time under different signal bandwidth, carrier frequency and length (see table 1, as well as loop 1 in Figure 3).
- 2) Simulate the acquisition of bistatic radar echoes for a point target in the scene (see Figure 2 and loop 2 in Figure 3).
- Estimate the timedrift and initial offset from all sync. acquisitions and calculate the resulting estimation errors. The analysis thereof is given in Section III.
- 4) Insert these estimation errors into the bistatic compensation process and perform the full azimuth focusing via backprojection.
- 5) Inspect the focused scatterer return in terms of peak location error, 3dB mainlobe width (calculated at -3dB from the peak) and sidelobe ratio as shown in Section III.

III. SIMULATION RESULTS

The simulation described in Section II is performed with the parameters given in Table 1. Synchronisation signals are exchanged for the duration of the simulated radar operation and the time drift is estimated. Each run of the procedure in Figure 3 is repeated for 50 different random realisations of

Table 1. Simulation parameters

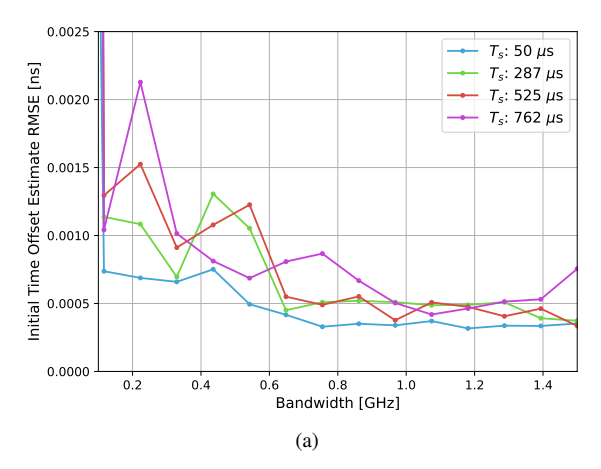
Parameter	Symbol	Value	Unit
Platform Altitude	$h_{1,2}$	100	m
Platform Velocity	$ v_{1,2} $	10	$\frac{m}{s}$
Radar Bandwidth	B_{rad}	2	GHz
Radar Carrier Freq,	$f_{c,rad}$	1	GHz
Radar Signal Duration	$T_{s,rad}$	1	ms
LO Frequency	f_{lo}	12	MHz
LO FreqOffset Range	Δf_{LO}	± 1	ppm
Sync. Bandwidth	B_{sync}	0.01-1.5	GHz
Sync. Signal Duration	$T_{s,sync}$	0.05 - 0.762	ms
CW Carrier	$f_{c,cw}$	0.5-3	GHz
No. Chirps	N_c	512	-

the simulated LO offsets as well as the initial timing offset to obtain a statistical performance metric.

For the LFM waveforms, the estimation results from upand down chirps are averaged and the Root Mean Squared Error (RMSE) is shown for the initial timing offset estimate and the time drift estimate in Figures 4a and 4b, respectively. By inspecting the errors of both estimated quantities, it is clearly visible that the error is reduced for increasing bandwidth. This is expected, since the resolution of an FMCW system is inversely proportional to the bandwidth with $\delta = c/2B$ [18]. However, it is also visible that the shorter waveforms tend to produce a smaller estimation error than longer chirp durations. This can likely be explained by the effects of the timing drift on the ramp rate of the signal. Due to the slightly different sampling frequencies in both radars Digital to Analog Converters (DACs) and Analog to Digital Converters (ADCs), the signal experiences a squash or stretch, which leads to an offset in the ramp rate. Upon deramping in the bistatic receiver, a residual frequency modulation remains in the beatsignal, smearing and shifting the frequency peak of the FFT. This shift causes an error in the estimation of the initial time offset and can only approximately be corrected. Since this effect becomes more severe for large chirp durations and increasing bandwidth, short chirps with high bandwidths may have an advantage when this estimation method is used.

Figure 5 shows the timedrift estimation based on a CW signal exchange. Contrary to the LFM signal, here an improvement is visible with increasing signal length, wich is generally in accordance with the theoretical expectations for frequency estimation. However, the overal estimation performance is worse, since the frequency resolution in the CW case scales with the signal duration $\propto 1/T_s$, while the resolution in the LFM case scales with the signal bandwidth $\propto c/B$. The choice of waveform and the achievable time estimation performance is ultimatively guided by the synchronisation requirements for the radar system. For example, for an L-band system $(f_c=1.325~{\rm GHz})$ the time synchronisation should be better than $\pm 10.5~{\rm ps}$ for interferometric applications [20].

The simulated estimation errors are then used as a reference to investigate how they impact the bistatic SAR imaging.



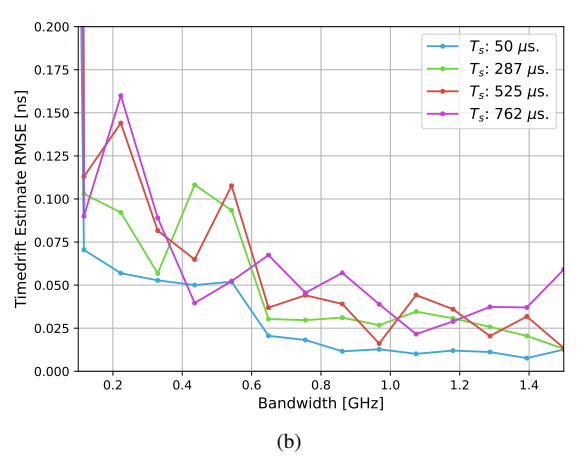


Fig. 4. Up- and Downchirp parameter estimation: (a) Initial time offset estimate; (b) time drift estimate

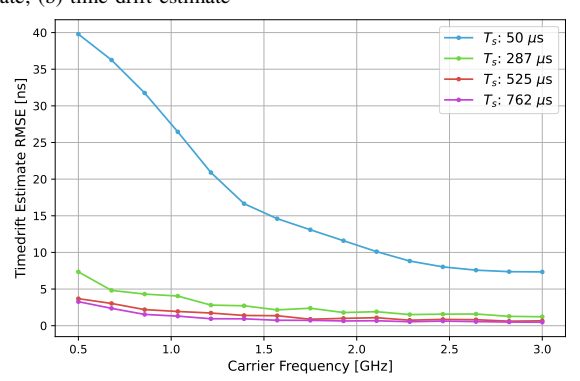


Fig. 5. Timedrift estimation based on a CW signal with increasing carrier and length

Image focusing is done via the backprojection algorithm [19], after corrections based on the offset estimates have been made. An increasing error is assumed for this correction step. To examine the influence on the image, a point target was placed in the scene center, corresponding to ≈ 130 m slantrange to the radar at the zero-Doppler point. After backprojection, a cut along range and azimuth over the target response is extracted to analyse the mainlobe width and thereby the resolution, shown in Figure 6. The fluctuations are presumed to come from numerical errors in the process extracting the mainlobe width. Besides those numerical errors, the resolution shows

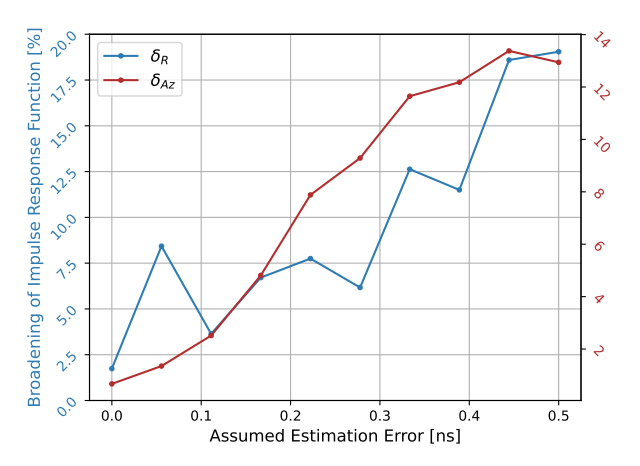


Fig. 6. Deterioration of range (blue) and azimuth (red) resolution w.r.t. the theoretical achievalble resolution after SAR focusing if no errors are present.

a worsening with higher estimation erros, as it would be expected.

IV. CONCLUSIONS AND OUTLOOK

The developed simulation framework offers an extensible platform for the investigation of different waveforms and synchronisation schemes that will be further expanded to fully analyse the possibilities of arbitrary waveform generation and exchange for the means of synchronisation. This work so far has shown the impact of increasing signal duration and bandwidth on synchronisation error estimation using LFM and CW waveforms specifically with respect to the timing offsets and drifts. It has been identified, that larger time and bandwidth combinations may produce extra errors in the parameter estimation due to spectral smearing of the focused peak. This of course is only an effect impacting LFM signals. A sweet spot between resolution, received energy and time-bandwidth product may have to be found that suits the system requirements.

There is a vast range of possible methods that could be employed on a digital, software-defined and reconfigurable direct RF radar system for both synchronisation and radiometric sensing not only limited to the here shown concepts. Such concepts with the focus on multistatic SAR processing will be further explored in future work. Bistatic measurements with AMD's (former Xilinx) Radio Frequency System on Chip (RFSoC) devices are currently in process and are aimed to be included in the final paper submission.

REFERENCES

- [1] G. Krieger and A. Moreira, "Spaceborne bi- and multistatic SAR: Potential and challenges," *IEE Proceedings Radar, Sonar and Navigation*, vol. 153, no. 3, p. 184, 2006, ISSN: 1350-2395. DOI: 10. 1049/ip-rsn:20045111.
- [2] G. Krieger and M. Younis, "Impact of Oscillator Noise in Bistatic and Multistatic sar," *IEEE Geoscience and Remote Sensing Letters*, vol. 3, no. 3, pp. 424–428, 2006. DOI: 10.1109/LGRS.2006.874164.
- [3] R. Ghasemi, T. Koegel, P. Fenske, R. Schober, and M. Vossiek, "Time and Frequency Synchronization for Real-Time Wireless Digital Communication Systems," in 2024 15th German Microwave Conference (GeMiC), IEEE, Mar. 2024, pp. 13–16. DOI: 10.23919/ gemic59120.2024.10485238.

- [4] J. M. Merlo, S. R. Mghabghab, and J. A. Nanzer, "Wireless Picosecond Time Synchronization for Distributed Antenna Arrays," *IEEE Transactions on Microwave Theory and Techniques*, vol. 71, no. 4, pp. 1720–1731, Apr. 2023, ISSN: 1557-9670. DOI: 10.1109/ tmtt.2022.3227878.
- [5] S. Prager, M. S. Haynes, and M. Moghaddam, "Wireless Subnanosecond RF Synchronization for Distributed Ultrawideband Software-Defined Radar Networks," *IEEE Transactions on Microwave Theory and Techniques*, vol. 68, no. 11, pp. 4787–4804, Nov. 2020, ISSN: 1557-9670. DOI: 10.1109/tmtt.2020.3014876.
- [6] M. Younis, R. Metzig, G. Krieger, M. Bachmann, and R. Klein, "Performance Prediction and Verification for the Synchronization Link of TanDEM-X," in 2007 IEEE International Geoscience and Remote Sensing Symposium, 2007, pp. 5206–5209. DOI: 10.1109/IGARSS. 2007 4424035
- [7] M. Stefko, O. Frey, C. Werner, and I. Hajnsek, "Calibration and Operation of a Bistatic Real-Aperture Polarimetric-Interferometric Ku-Band Radar," *IEEE Transactions on Geoscience and Remote Sensing*, vol. 60, pp. 1–19, 2022. DOI: 10.1109/TGRS.2021.3121466.
- [8] M. Ash, M. Ritchie, K. Chetty, and P. V. Brennan, "A New Multistatic FMCW Radar Architecture by Over-the-Air Deramping," *IEEE Sensors Journal*, vol. 15, no. 12, pp. 7045–7053, 2015. DOI: 10.1109/JSEN. 2015.2466477.
- [9] D. Werbunat et al., "On the Synchronization of Uncoupled Multistatic PMCW Radars," *IEEE Transactions on Microwave Theory and Techniques*, vol. 72, no. 8, pp. 4932–4944, 2024. DOI: 10.1109/TMTT. 2024.3359035.
- [10] M. Gottinger, F. Kirsch, P. Gulden, and M. Vossiek, "Coherent Full-Duplex Double-Sided Two-Way Ranging and Velocity Measurement Between Separate Incoherent Radio Units," *IEEE Transactions on Microwave Theory and Techniques*, vol. 67, no. 5, pp. 2045–2061, 2019. DOI: 10.1109/TMTT.2019.2902553.
- [11] P. Fenske, T. Koegel, R. Ghasemi, and M. Vossiek, "Constellation Estimation, Coherent Signal Processing, and Multiperspective Imaging in an Uncoupled Bistatic Cooperative Radar Network," *IEEE Journal* of Microwaves, vol. 4, no. 3, pp. 486–500, Jul. 2024, ISSN: 2692-8388. DOI: 10.1109/jmw.2024.3393120.
- [12] Y. Wang et al., "First Demonstration of Single-Pass Distributed SAR Tomographic Imaging With a P-Band UAV SAR Prototype," *IEEE Transactions on Geoscience and Remote Sensing*, vol. 60, pp. 1–18, 2022. DOI: 10.1109/TGRS.2022.3221859.
- [13] M. Eineder, "Ocillator clock drift compensation in bistatic interferometric SAR," in *IGARSS 2003. 2003 IEEE International Geoscience and Remote Sensing Symposium. Proceedings (IEEE Cat. No.03CH37477)*, ser. IGARSS-03, vol. 3, IEEE, pp. 1449–1451. DOI: 10.1109/igarss.2003.1294140.
- [14] N. Ustalli, G. Krieger, J. Mittermayer, M. Villano, and C. Waldschmidt, "Mirrorsar Concept: Phase Synchronization Analysis," in 2022 Kleinheubach Conference, 2022, pp. 1–4.
 [15] A. Grathwohl, B. Meinecke, M. Widmann, J. Kanz, and C.
- [15] A. Grathwohl, B. Meinecke, M. Widmann, J. Kanz, and C. Waldschmidt, "UAV-Based Bistatic SAR-Imaging Using a Stationary Repeater," *IEEE Journal of Microwaves*, vol. 3, no. 2, pp. 625–634, 2023. DOI: 10.1109/JMW.2023.3253667.
- [16] E. Rodrigues-Silva, M. Rodriguez-Cassola, G. Krieger, and A. Moreira, "GNSS-Based Phase Synchronization for Bistatic and Multistatic Synthetic Aperture Radar," *IEEE Transactions on Geoscience and Remote Sensing*, vol. 62, pp. 1–14, 2024. DOI: 10.1109/TGRS.2024. 3406797.
- [17] U. Jayamohan, "Not Your Grandfather's ADC: RF Sampling ADCs Offer Advantages in Systems Design," 2015. [Online]. Available: https://api.semanticscholar.org/CorpusID:36135912.
- [18] S. M. Patole, M. Torlak, D. Wang, and M. Ali, "Automotive radars: A review of signal processing techniques," *IEEE Signal Processing Magazine*, vol. 34, no. 2, pp. 22–35, 2017. DOI: 10.1109/MSP.2016. 2628914.
- [19] L. A. Gorham and L. J. Moore, "SAR image formation toolbox for MATLAB," in *Algorithms for Synthetic Aperture Radar Imagery XVII*, E. G. Zelnio and F. D. Garber, Eds., SPIE, Apr. 2010. DOI: 10.1117/ 12.855375.
- [20] S. Dunkel and E. Schreiber, "Phase Synchronization Concept for the Bistatic Extension of the Airborne F-SAR System," in 2024 Kleinheubach Conference, 2024, pp. 1–4. DOI: 10.23919 / IEEECONF64570.2024.10738977.